CrossMark

An Investigation of the Seismic Behaviour of an Ancient Masonry Bastion Using Non-Destructive and Numerical Methods

A.C. Altunisik[1] · S. Adanur[1] · A.F. Genc[1] · M. Gunaydin[2] · F.Y. Okur[1]

Abstract Determining the structural behavior of masonry structures is a challenge due to their lack of homogeneity. The seismic behavior of masonry structures is especially complex. The aim of this study was to examine the structural behavior of Zağanos Bastion using both experimental and numerical methods. The Operational Modal Analysis technique, including the Enhanced Frequency Domain Decomposition Method, and the Stochastic Subspace Identification Method were used to illustrate experimentally the dynamic characteristic of the bastion. A finite element model was developed using ANSYS software in order that the dynamic characteristics of the bastion, including natural frequencies and mode shapes, could be calculated numerically. Seismic analysis was carried out using the 1999 Kocaeli earthquake ground motion record to determine the linear and nonlinear seismic behavior of the bastion. The Turkish Earthquake Code and its general technical specifications were used to evaluate the seismic results. The results show that the maximum and minimum principal stresses exerted on the masonry components exceeded the code requirements at some points, but in general the requirements for the stresses were satisfied.

Introduction

Historical buildings play an important role in the cultural heritage of most nations. As works of art they contribute hugely to the beauty of the built environment and are crucial to many cities and countries in attracting tourism. For this reason, many countries have introduced regulations for the conservation of their historic structures.

Many historic structures were built with stone and mortar using masonry techniques. Masonry was a common construction technique in ancient times. Despite consisting of only a few materials, namely stone, mortar and timber block, it is often difficult to understand the actual behaviour of masonry structures. This is because of the non-homogeneity and anisotropic forms of the material properties. Through time, steel and concrete materials took the place of masonry in construction. Although many have been lost over the years, large numbers of masonry historic structures survived, and some of them are still in service. However, this part of our cultural heritage is seriously threatened by both natural and manmade forces over the course of time [1].

Masonry structures can be exposed to many different forces such as earthquakes, floods, fires, wars and damage through vandalism, and also to deterioration in the strength of construction materials, support settlement, time-dependent

✉ A. C. Altunisik
ahmetcan8284@hotmail.com

S. Adanur
sadanur@ktu.edu.tr

A. F. Genc
af.genc@ktu.edu.tr

M. Gunaydin
gunaydin61@hotmail.com.tr

F. Y. Okur
yesevi@ktu.edu.tr

1 Department of Civil Engineering, Karadeniz Technical University, 61080 Trabzon, Turkey

2 Department of Civil Engineering, Gümüşhane University, Gümüşhane, Turkey

deformations, and excessive and irregular loading due to inappropriate use [2]. Masonry structures are highly vulnerable to dynamic actions, particularly seismic ones [3]. This is due to the structure of the masonry which has low tensile strength, and is primarily designed to resist compressive stresses. They can be easily damaged or even destroyed through tensile stresses. Therefore, it is important that the seismic behavior of masonry structures is investigated in detail.

Determining the structural behaviour of historical masonry structures is very difficult due to uncertainties related to material properties, the complex interaction between structural elements, and the lack of historical documentation. The Finite Element Method (FEM) was used to determine numerically the structural behavior of engineering structures. Static, dynamic, linear and nonlinear behavior can be examined using the FEM, but it may not be sufficient on its own to identify the seismic behavior of masonry structures because of some difficulties with the model in relation to material characteristics, boundary conditions, meshing sizes, etc. [4]. In the light of these difficulties, the FE model should be verified using experimental methods to determine the actual behavior of the structures.

There are currently two experimental methods (a) Experimental Modal Analysis (EMA) and (b) Operational Modal Analysis (OMA), which are commonly used to determine the dynamic characteristics of structures. In EMA, analyses are made with a known excitation force generated by a shaker, then the structural response measured. However, in OMA, structures are vibrated by environmental and operational loads, and then the structural response is measured. The authors believe that OMA is more appropriate than EMA for identifying the dynamic characteristics of historical structures than EMA because OMA better represents real operational conditions [5]. OMA is also more appropriate for historic structures, because it is a totally non-destructive testing method [6].

There are many studies in the literature about historical masonry structures. Almost every aspect of the subject has been examined experimentally and numerically. Historical masonry arch bridges [7–9], towers [10–12], minarets [13, 14], mosques [15, 16], churches [17–19], chimneys [20] etc. have all been investigated by different authors. Very rigid structures such as castles, fortresses and bastions have been investigated in terms of static and dynamic structural behavior [21–27]. But aside from these studies, there has not been enough investigation in relation to OMA, finite element models, and in particular, the seismic behavior of these structures.

Historical masonry structures reflect the historical texture of cities. Castles, fortresses and bastions are often the first historical structures that draw the attention of the visitor to a city. These

Fig. 1 Pictures of Zağanos Bastion

buildings hold a substantial place in cultural heritage and require structural investigation and conservation. In the literature they are often the subject of investigation in terms of static and dynamic behaviors. However, there are few studies in the literature which include both numerical and experimental seismic investigation of castles, fortresses and bastions.

In this paper, the numerical-experimental dynamic characteristics and seismic behavior of an ancient bastion were investigated. Dynamic characteristics of the bastion were first obtained by OMA and FEM. The experimental modal parameters were identified using both Enhanced Frequency Domain Decomposition (EFDD) and Subspace Structural Identification (SSI) techniques. Then linear and nonlinear seismic analysis was carried out and the results from the experimental and numerical methods were examined to determine the structural behavior of the bastion.

Zağanos Bastion

The castle at Trabzon dates back to ancient times, but first repairs and expansions were made during the Byzantine period in the sixth century. After the Byzantines, the Ottomans
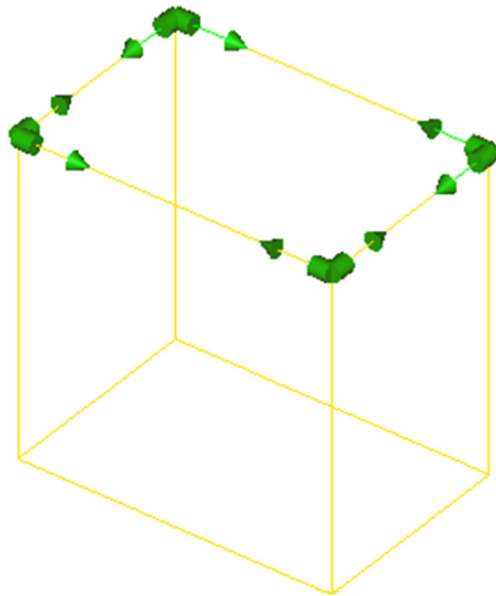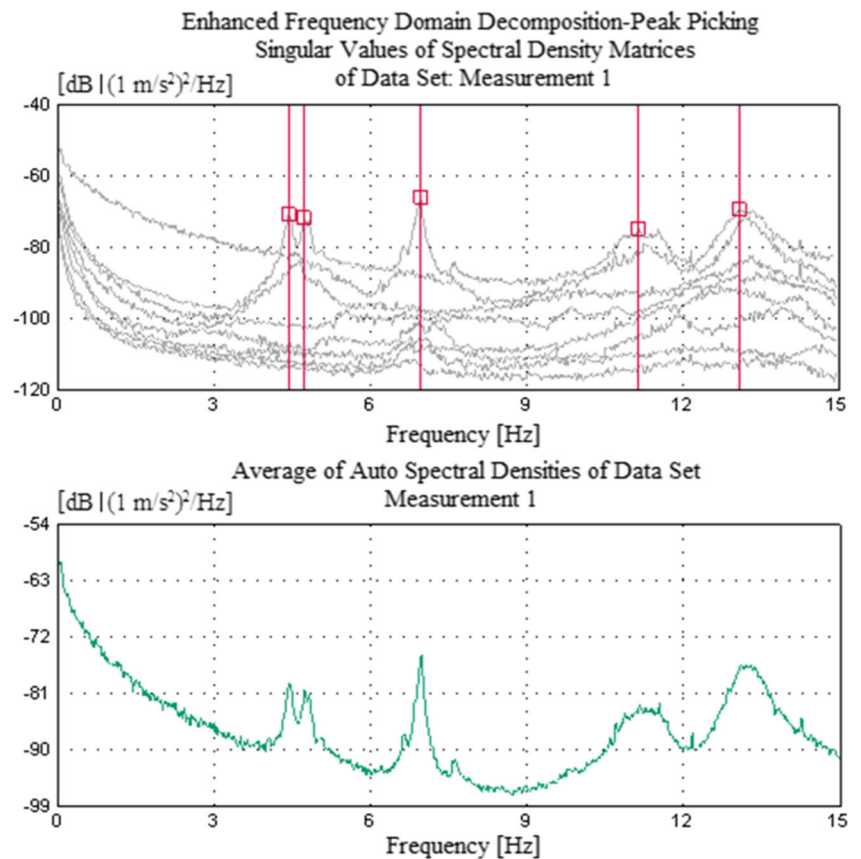

Fig. 2 The accelerometer connections

Fig. 3 Bastion model and accelerometer layout used in the ambient vibration test

continued to repair and expand the castle until the eighteenth century, when the castle took on its current form. The centre of the city and government buildings were located within the castle in the Byzantine and Ottoman periods.

The Zağanos bastion was located in the middle part of the castle. It was constructed from brown conglomerate stone. The masonry technique used in the bastion was different from other parts of the castle. The stones were arranged in a linear line, and there was no mortar in the wall. The stones were used as bond and stretcher stones. In the last century, some additional features such as an elevator, RC floor and cement based mortar were added which undermined the authenticity of the original structure. The structural system of the bastion is based on load-bearing walls, vaults and arches. It is approximately 17 m in height, 15 m wide and 10 m deep. The thickness of the bastion walls is approximately 2.55 m from ground to the middle of the bastion, and 1.25 m from the middle to the top. The bastion has two main storeys which have vault roofs and they were divided into two parts with RC floors, thus four storeys were obtained. Some pictures of the bastion are given in Fig. 1.

Experimental Response of the Bastion

An ambient vibration test was performed on the bastion to determine its dynamic characteristics such as natural frequencies, mode shapes and damping ratios. In the ambient vibration test, a B&K 3560 data acquisition system with 17 channels and B&K 8340-type uni-axial accelerometers with 10 V/

Fig. 4 SVSDM (**a**) and AASD (**b**) of the data set

Fig. 5 The stabilization diagram (a) and singular values (b) for the first three modes
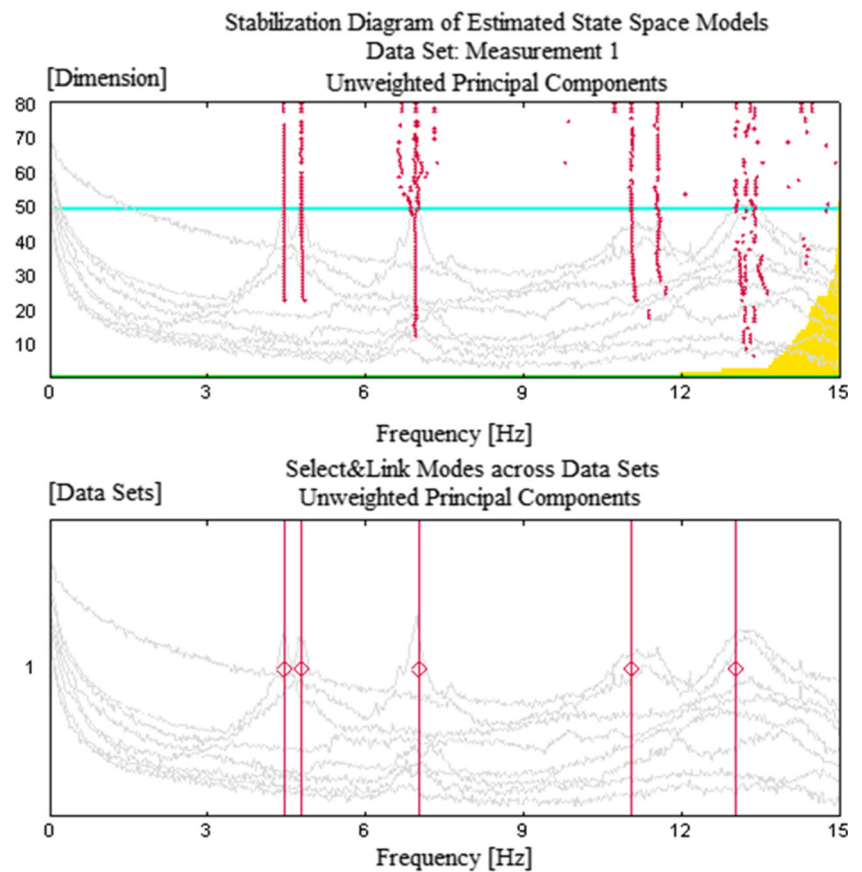
g sensitivity, uni-axial signal cables, PULSE and OMA software were used as the test equipment. The frequency range was selected as 0-15 Hz and eight accelerometers were located at the top of the bastion in transverse and longitudinal directions (Fig. 2).

Ambient vibration testing was carried out for 45 min at a very low level of vibration. The signals obtained from the accelerometers were accumulated in a Brüel&Kjaer 3560 data acquisition system and then were transferred into the PULSE software [28]. After the test, the signals were transmitted to the OMA software [29] for signal processing. Then, modal parameters were extracted using EFDD and SSI techniques. A representative model generated in PULSE software for the bastion and accelerometers layout, along with their directions, are presented in Fig. 3.

The dynamic characteristics of the bastion were extracted using both the EFDD and SSI techniques after signal processing.

Singular values of the spectral density matrices (SVSDM) of the data set and the average of the auto spectral densities (AASD)

Fig. 6 The mode shapes of the bastion

Mode 1 (Transverse Mode)   Mode 2 (Longitudinal Mode)   Mode 3 (Torsional Mode)
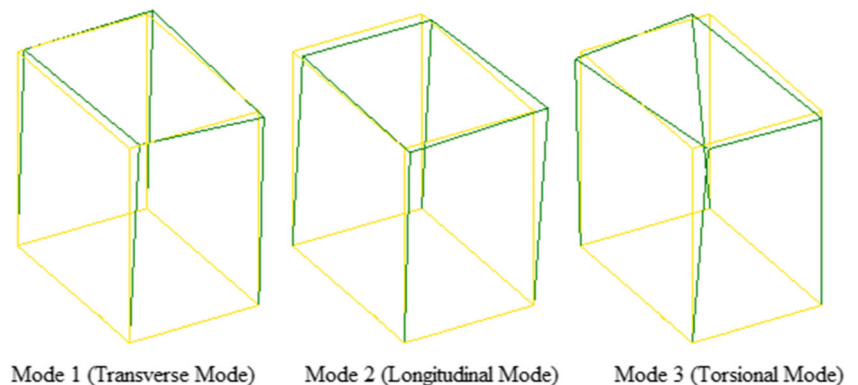
of the data set obtained by EFDD technique for the bastion are given in Fig. 4. As shown, the first three natural frequencies are obtained between the 0 and 15 Hz frequency range.

The dynamic characteristics of the bastion were also identified using the SSI technique. The stabilization diagram and singular values for the first three modes are given in Fig. 5. For signal processing control, maximum state space dimension to estimate is selected as 80. The automatic model estimation option was chosen using Unweighted Principal Component (UPC) estimators with values of 1, 80, and 1 for start, stop and increment, respectively. The natural frequencies, mode shapes and modal damping ratios were calculated using the stable values. The stability of the poles is often evaluated in terms of the variability of three parameters - frequency, modal shape and damping ratio - throughout model order variations. As can be seen in Fig. 5, three natural frequencies are also identified between 0 and 15 Hz. Figure 6 illustrates the first three mode shapes. The first one is transverse mode, the second is longitudinal mode, and the third is torsional mode.

The modal assurance criterion (MAC) graphics are widely plotted to determine the correlation between the mode shapes. The MAC values are defined as a scalar constant relating the degree of consistency (linearity) between one modal and another reference modal vector [30] as follows:

$$MAC = \frac{\left|\{\phi_{ai}\}^{\mathrm{T}}\{\phi_{ej}\}\right|^2}{\{\phi_{ai}\}^{\mathrm{T}}\{\phi_{ai}\}\{\phi_{ej}\}^{\mathrm{T}}\{\phi_{ej}\}}, \tag{1}$$

where $\{\phi_{ai}\}$ and $\{\phi_{ej}\}$ are the modal vectors of ith and jth for different techniques, respectively.
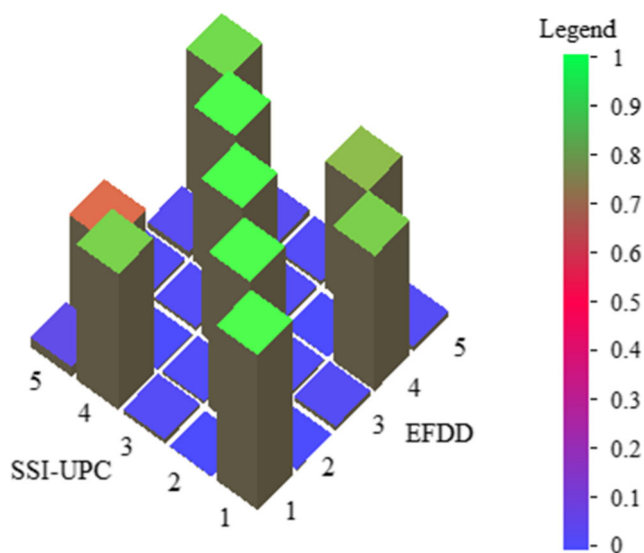
Table 1 Modal Parameters of the bastion for EFDD and SSI

Mode	Frequency (Hz)			Damping Ratios (%)		
	EFDD	SSI	Diff.(%)	EFDD	SSI	Diff.(%)
1	4.455	4.452	0.07	1.3500	1.235	8.52
2	4.750	4.787	0.77	0.7535	2.165	65.2
3	6.967	7.011	0.63	0.6241	1.110	43.7

The graphics were automatically constituted by OMA software using Eq. 1. Figure 7 shows the MAC graphics estimated by using EFDD and SSI techniques for the three mode shapes. Figure 7 shows that the correlation between the mode shapes reflected by MAC values seems very good. The MAC values located on the diagonals were obtained as nearly one. This means that there is a close agreement between results and the EFDD and SSI results are almost overlapping. The other values (except diagonal) were attained as nearly zero.
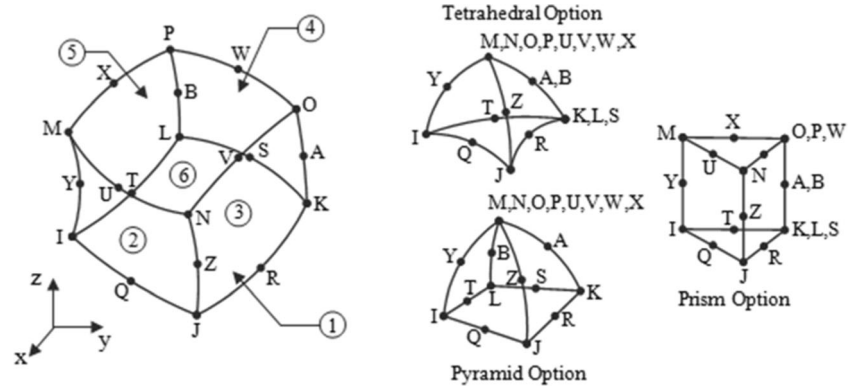
The experimental dynamic characteristics of the bastion identified using both EFDD and SSI techniques are compared in Table 1. The natural frequencies were calculated within 4.455 Hz–6.967 Hz and 4.452 Hz–7.011 Hz respectively for the EFDD and SSI techniques. In addition, the damping ratios were identified within 0.6241 %–1.350 % and 1.110–2.165 for EFDD and SSI, respectively. It can be seen that there is an excellent agreement between the natural frequencies, with a maximum error of 0.77 % in the second mode. However, there is no significant agreement between the damping ratios.

Numerical Analyses

A finite element model of the Zağanos bastion was constituted with ANSYS software [31]. In the finite element model of the bastion, SOLID186 solid element was used. This element has 20 nodes and three degrees of freedom per node namely translations in nodal x, y and z directions. The element has the capability of plasticity, elasticity, creep, stress stiffening, large deflection, and large strains. In addition, the element has tetrahedral, pyramid or prism options for meshing, and these options provide easy meshing for models [31]. A schematic picture of SOLID186 is given in Fig. 8. Building survey drawings of the bastion used in the FE modeling are given in Fig. 9.

The finite element model of the bastion includes 105,848 nodes and 67,289 solid elements. The supports of the bastion are assumed to be fixed in the model. The finite element model of the bastion is shown in Fig. 10.

Fig. 7 Modal assurance criterion correlation obtained from experimental measurement

Fig. 8 SOLID186 element

Four different structural element components exist in the FE model of the bastion, namely masonry walls, masonry arches and vault, reinforced concrete (RC) floors, and steel columns. There has been no experimental study with regard to the material characteristic of the bastion. The material characteristics are taken to be similar to those available in the literature. In the literature, different material properties are used for masonry structures [12, 32–34]. In can be seen that the modulus of elasticity is in the range from 1.5E9N/m² to 5.0E9N/m² and the density in the range from 1600 kg/m³ to 2200 kg/m³. Therefore, the material properties of masonry elements given in Table 2 are selected from between these ranges.

Results of the FE analyses for the bastion are evaluated according to the Turkish Earthquake Code, Chapter 5.3 (compression safety stress of walls where free compression stress is unknown) [35].

The compression safety stress is selected as 0.3 MPa from the code for masonry walls in which free compression stress is unknown. This value defines stone walls which are bonded with lime mortar supported with cement. In the time history analysis, there is no reduction factor for the earthquake load, therefore the safety stresses are magnified by 3 in the calculations.
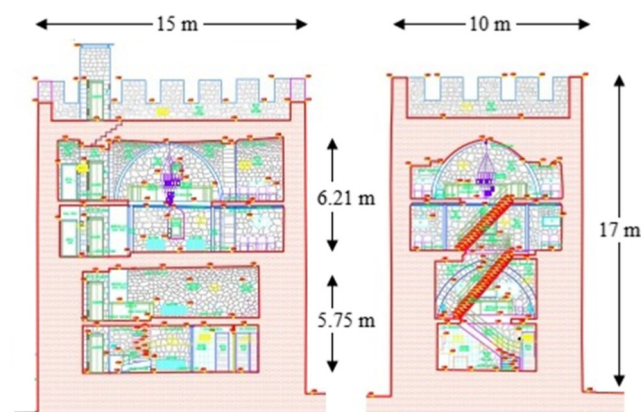

Fig. 9 Rilievo drawings of the bastion

The compression safety stress value for the stone material is calculated as;

$$f_s = 0.3*3$$
$$= 0.9 MPa \qquad \text{(Stone, used in walls, arches and vaults)}$$

The tension safety stresses can be taken as 15 % of the compression safety stresses [36, 37], thus,

$$f_s = 0.9*0.15$$
$$= 0.135 MPa \qquad \text{(Stone, used in walls, arches and vaults)}$$

Safety stresses for the materials used in the Zağanos Bastion are given in Table 3. These are bottom limits for the masonry material in the code and allowable stress design takes account of the safety strengths.

Modal Analysis

The dynamic characteristics of the bastion were extracted from the FE modal analysis. The first three frequencies were obtained as 5.9467 Hz, 6.5856 Hz and 9.4640 Hz, respectively. Mode shapes of the bastion appear as transverse, longitudinal and torsional modes, respectively. The frequency values and corresponding mode shapes are shown in Fig. 11. A contour plots refer to modal displacements. Experimental and analytical modal displacements were used to obtain the MAC values. Experimental and numerical natural frequencies are given in Table 4. The maximum difference between the frequencies was obtained as 26 %.

Time-History Seismic Analyses

Linear Time-History Seismic Analysis

The structural behavior of the bastion was examined under seismic load using time-history analysis. The horizontal component (KOCAELI_DZC270) of the 1999 Kocaeli earthquake obtained from Duzce station was selected for the analyses

Fig. 10 Views and sections of the finite element model of the bastion
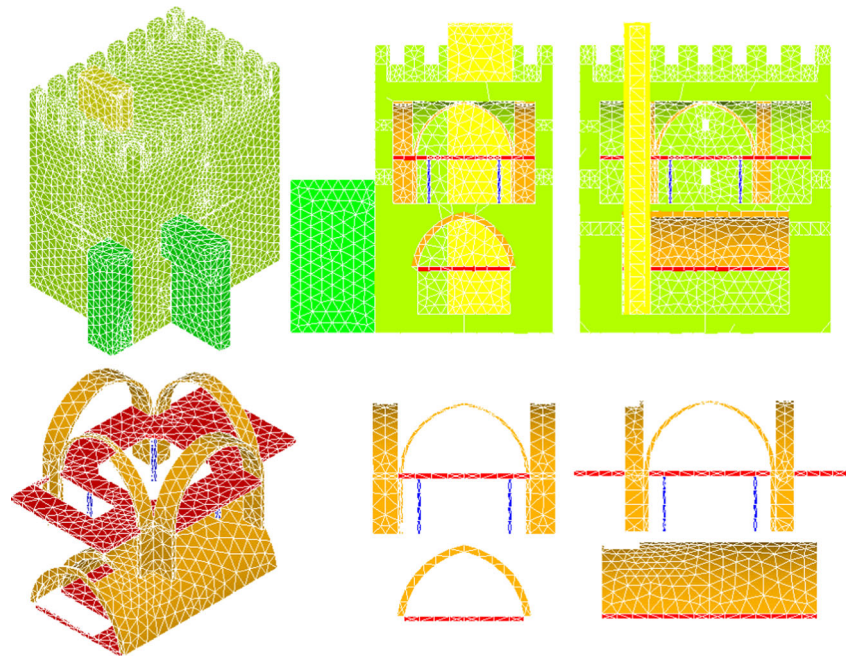
[38]. The time-histories of the record with 0.364 g peak ground acceleration is given in Fig. 12. Only the time between 5 and-10 s of the earthquake motion, which is the most effective duration, was taken into account. This was because of the computational demand of this method and because it was less time consuming.

After the experimental and analytical calculations, it can be seen that the first and second modes are obtained on the x (transverse) and y (longitudinal) directions with similar frequency values, respectively. So, it can be said that the bastion has the same lateral stiffness in both directions. In the seismic analysis, one component of acceleration (KOCAELI_DZC270) was considered and applied to the bastion at first mode direction (x-transverse direction) to obtain the most unfavorable condition.

The maximum displacement contour diagram for the bastion is given in Fig. 13. The maximum displacement occurs at the upper part of the bastion with a value of 7.8 mm. Also, the displacements decrease towards the lower part of the bastion.

The stress results of the bastion are given as principal stresses. According to the stress results, it is possible that some failure and cracks will occur at the maximum stress points if the stresses reach the material strength, but the cracks cannot be seen in the linear analysis. The maximum and minimum principal stresses contour diagram of the bastion is given in Fig. 14. The maximum principal stress occurs on the RC floor locally with a value of 4.56 MPa. However, this value does not reflect the actual behavior of the bastion because the RC floor is not a main component of the bastion. The maximum principal stress found for the masonry components was 2.63 MPa and this occurred only at a localized point of the arch. Except for this localized stress, the maximum principal stresses were generally obtained as 0.93 MPa on the bastion. The minimum principal stress occurred on the RC floor locally with a value of 6.04 MPa. Also, the minimum principal stress occurring on the masonry components was 5.0 MPa. The main structural

Table 2 Linear material properties of the bastion used in the FE analyses

Elements	Material properties		
	Modulus of Elasticity (N/m^2)	Poisson Ratio (−)	Density (kg/m^3)
Masonry walls	2.4E9	0.2	2200
Masonry Arches and vault	4.0E9	0.2	2200
RC floors	2.5E10	0.2	2500
Steel column	2.0E11	0.3	7856

Table 3 Safety strength of materials

Materials	Material properties	
	Compression safety stress (MPa)	Tension safety stress (MPa)
Stone wall and arches	0.90	0.135

First Mode Transverse (*f=5.9467Hz*)

Second Mode Longitudinal (*f=6.5856Hz*)

Third Mode Torsion (*f=9.4640Hz*)

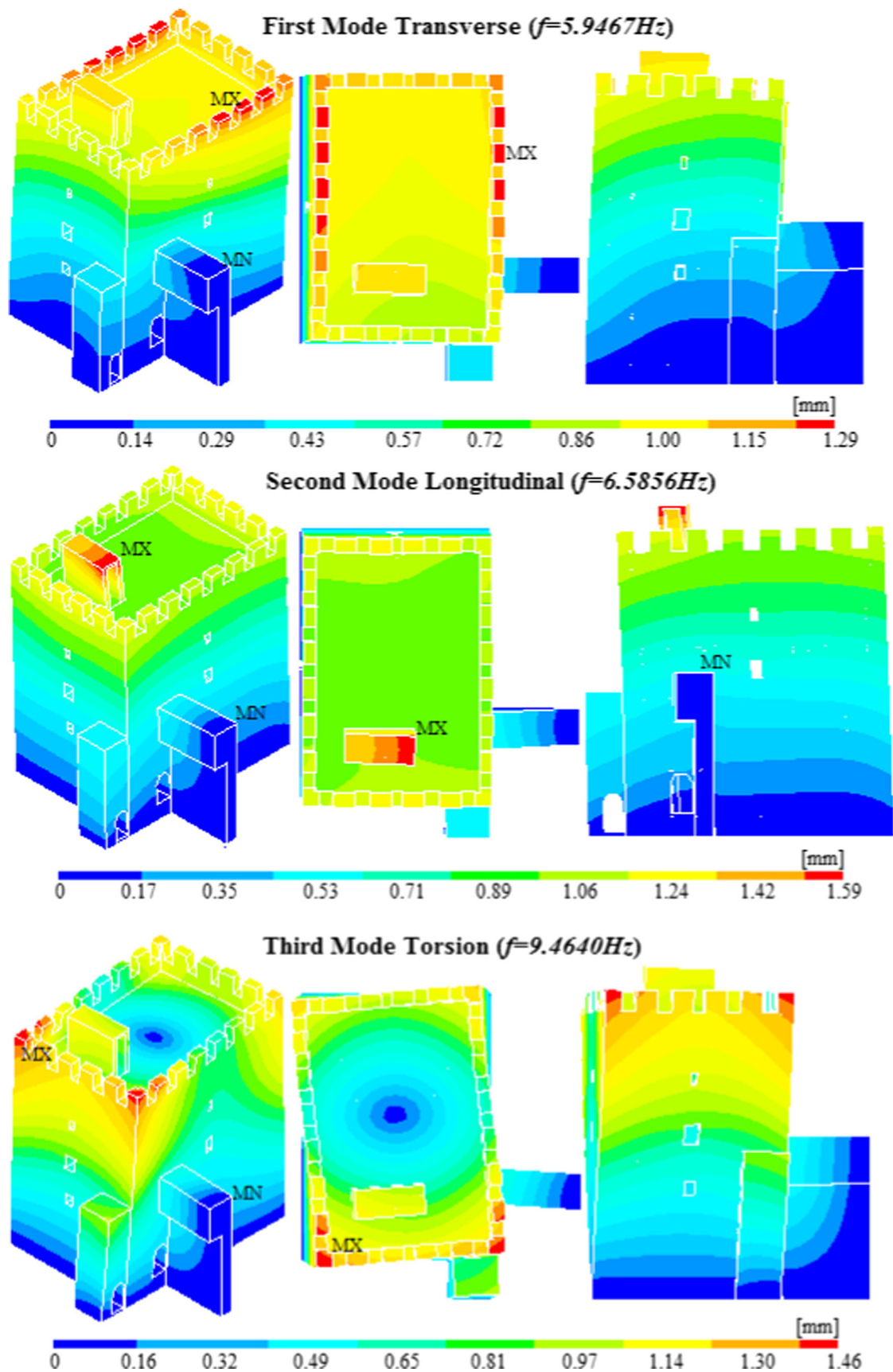**Fig. 11** First three mode shapes and frequencies

Table 4 Experimental and numerical natural frequencies

Mode	Frequency (Hz)		
	EFDD	SSI	Numerical
1	4.455	4.452	5.945
2	4.750	4.787	6.585
3	6.967	7.011	9.464

elements of the bastion showed a value of 0.90 MPa for compressive stress.

The maximum principal strain occurred at a point between the masonry arch and elevator wall. Maximum principal strain was obtained as 10.59E-4. The minimum principal strain occurred at the intersection of the masonry arch and the RC floor with a value of 19.47E-4. Also, the value of 8.60E-4 for minimum principal strain is obtained between the side rampart and the bastion area.

Results show that, structural components such as the elevator wall, RC floor and steel columns, which were added to the original structure at a later date, affect the structural behavior of the bastion. The maximum results were obtained for these elements. However, these results do not reflect the behavior of the entire structure. The main components of the bastion are the masonry walls, arches and vaults. These showed lower stress and strain values than the elements added later. Therefore, the maximum results obtained from the main component of the bastion are considered in the overall evaluation of structural behavior. The time history of displacement graphic is shown in Fig. 15.

Figure 16 gives a comparison of the maximum and minimum principal stress results which occurred at certain localized points of the bastion, the general stress results obtained for the masonry components of the bastion, and the code requirement. The maximum and minimum principal stresses which occurred between the element joints are higher than those for the code requirements. These are 0.9 MPa and 0.135 MPa for the minimum and maximum principal safety stresses, respectively. The minimum principal stresses obtained for the masonry components were generally lower than the code
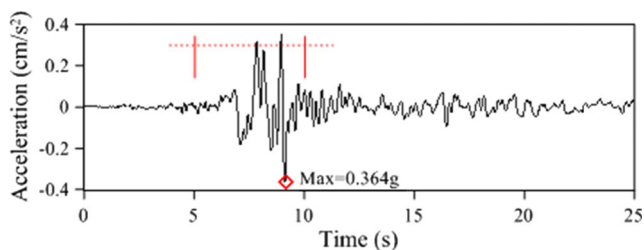
Fig. 12 The acceleration record of the Kocaeli (1999) earthquake horizontal component

requirements. However, maximum principal stresses exceeded the code requirements at several points.

The maximum local and non-structural stresses can only be obtained from the finite element analysis, due to such factors as irregular geometric shapes, and transition segments between different elements and strains. However these stress points are crucial if they occur at important points of the structure, such as on arches or vaults. Masonry structures are particularly vulnerable to maximum principal stresses but they can also carry high compressive stresses through the arches and vaults. Therefore the maximum principal stresses which occurred on the arches and vaults may be significant and must be given serious consideration.
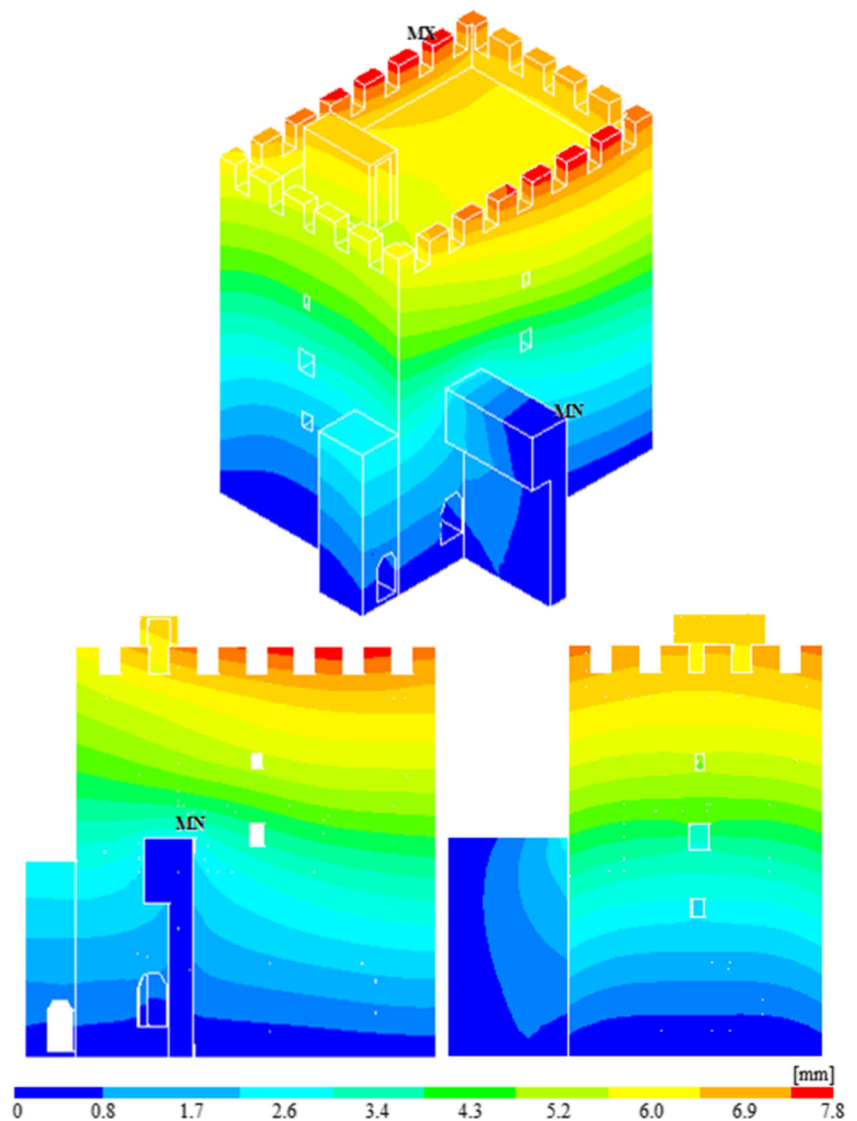
Nonlinear Time-History Seismic Analysis

After the linear seismic investigation, a nonlinear analysis was performed to complete the detailed examination of the bastion. The SOLID65 element type was used for the nonlinear analyses. This element has the capability of cracking (in three orthogonal directions), crushing, plastic deformation, and creep. The most important feature of this element is the treatment of nonlinear material properties [31]. In the study, nonlinear behavior is defined by the Drucker-Prager (DP) criterion with associated flow rule. Also, it is assumed that the failure surface is the Willam-Warnke (WW) surface. Nonlinear inputs were taken from the literature [39] and given in Table 5. The seismic acceleration record considered during the linear time-history analysis was defined for nonlinear analysis.

The Drucker-Prager yield surface was defined by two parameters; cohesion (c) and internal friction angle (φ). Also the Willam-Warnke failure surface was defined by two material constants; the uniaxial compressive strength f_c and the uniaxial tensile strength f_t, of the masonry [40].

The maximum displacements contour diagram obtained from the nonlinear seismic analysis is given in Fig. 17. The maximum displacement occurred at the upper part of the bastion, with a value of 35.7 mm. The displacements decreased towards the supports of the bastion.

The stress results of the bastion are given as principal stresses. According to the stress results, it is possible for some failure and cracks to occur at the maximum stress points if the stresses reach the material strength. The cracks can also be seen in the nonlinear analysis. In Fig. 18, the maximum and minimum principal stresses are presented. The maximum principal stress was obtained on the RC floor, with a value of 2.26 MPa. The stresses which occurred on the arches did not exceed the value of 0.49 MPa. Other than these points,

maximum principal stress did not exceed the value of
0.49 MPa at the bastion. The minimum principal stresses oc-
curred on the RC floor with a value of 4.81 MPa.
Stress points were found between the arch and elevator
with a value of 1.55 MPa. Apart from this, minimum
principal stresses did not exceed the value of 1.01 MPa
at the other arches. The minimum principal stresses
were not found to exceed the value of 1.01 MPa any-
where else in the bastion.

The maximum principal strains occurred between the arch
and the RC floor, the side rampart-bastion and near the
gate with a value of 15.74E-3. These results do not
exceed the value of 6.99E-3 on the other parts of the
bastion. The minimum principal strains occurred on the
arches with a value of 2.53E-3. Apart from this point,
the strains did not exceed the value of 0.54E-3. The
side rampart and lower parts of the bastion show a
strain value of almost 0.54E-3.

The cracking distributions of the bastion are given in
Fig. 19. Only cracking signs were observed. As shown in
Fig. 19, the cracks occurred generally in the lower part of
the bastion. Some damaged and cracked sections were also
detected near the windows and gate, side rampart, RC floors,
arches and vaults.

Comparison of Linear and Nonlinear Seismic Analyses Results

Linear and nonlinear seismic analyses results, such as
maximum displacements, and maximum and minimum
principal stresses and strains, are compared in Table 6.
It can be seen that the displacements, maximum and
minimum principal strains increase significantly in the
nonlinear analysis. The maximum and minimum princi-
pal stresses obtained from the linear analysis are greater
than those from the nonlinear analysis.

Fig. 14 Contour diagrams of the maximum and minimum principal stresses of the bastion from seismic analysis

a) Maximum principal stresses

b) Minimum principal stresses
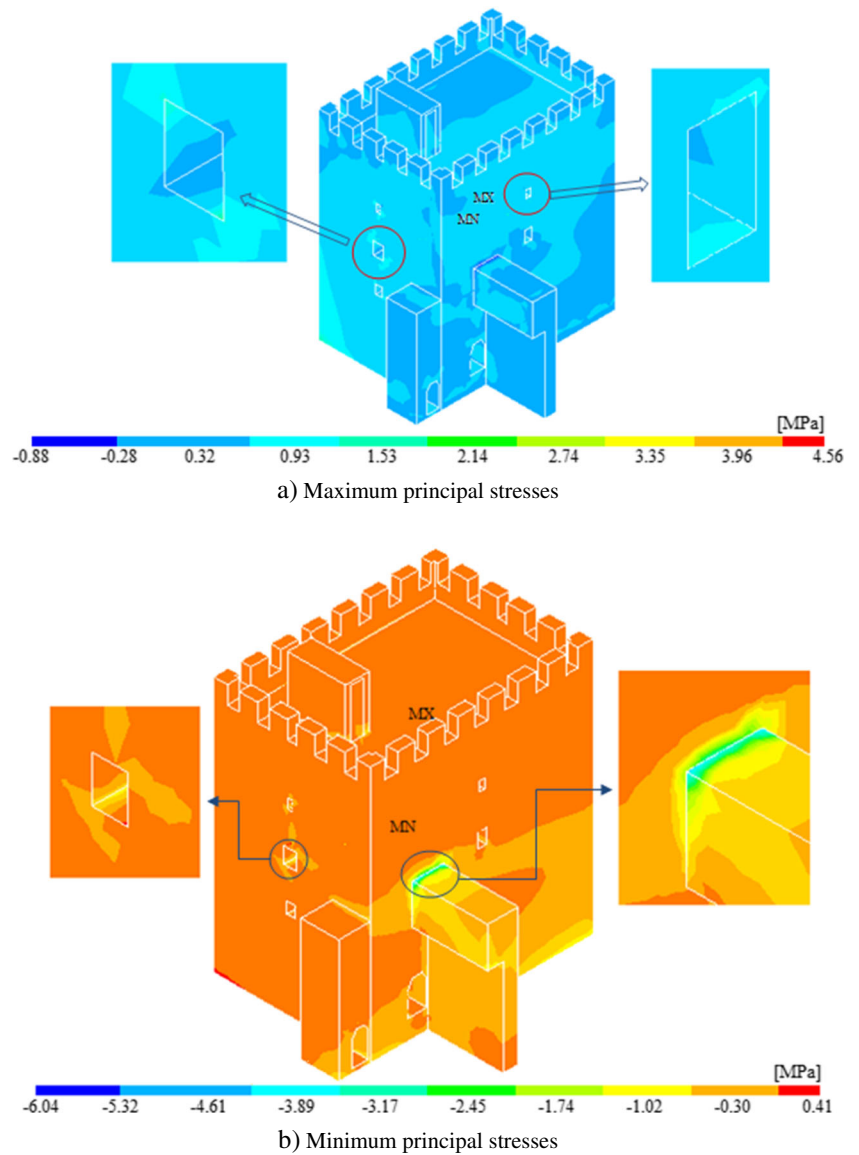
Conclusions

This paper presents findings from the FE modeling, modal testing and seismic behavior of Zağanos Bastion in Trabzon, Turkey. The dynamic characteristics of the bastion were determined numerically and experimentally. In the experimental measurements, EFDD and SSI modal parameter identification methods were employed to extract the dynamic
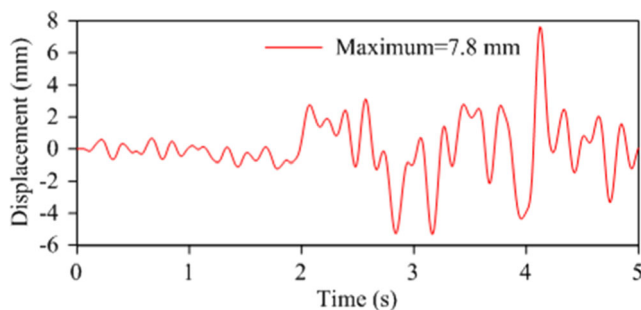

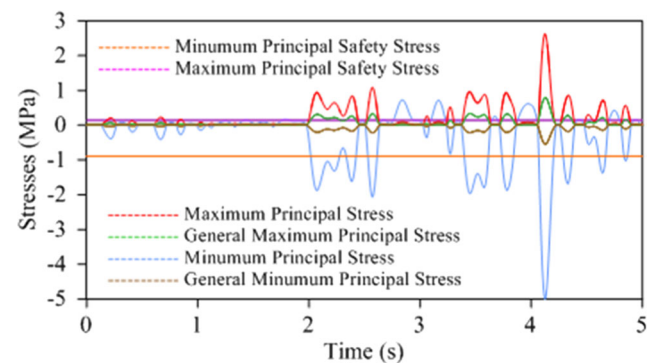**Fig. 15** Time-history lateral displacement graphic of the bastion

Fig. 16 Time-history stresses compared to the code restrictions

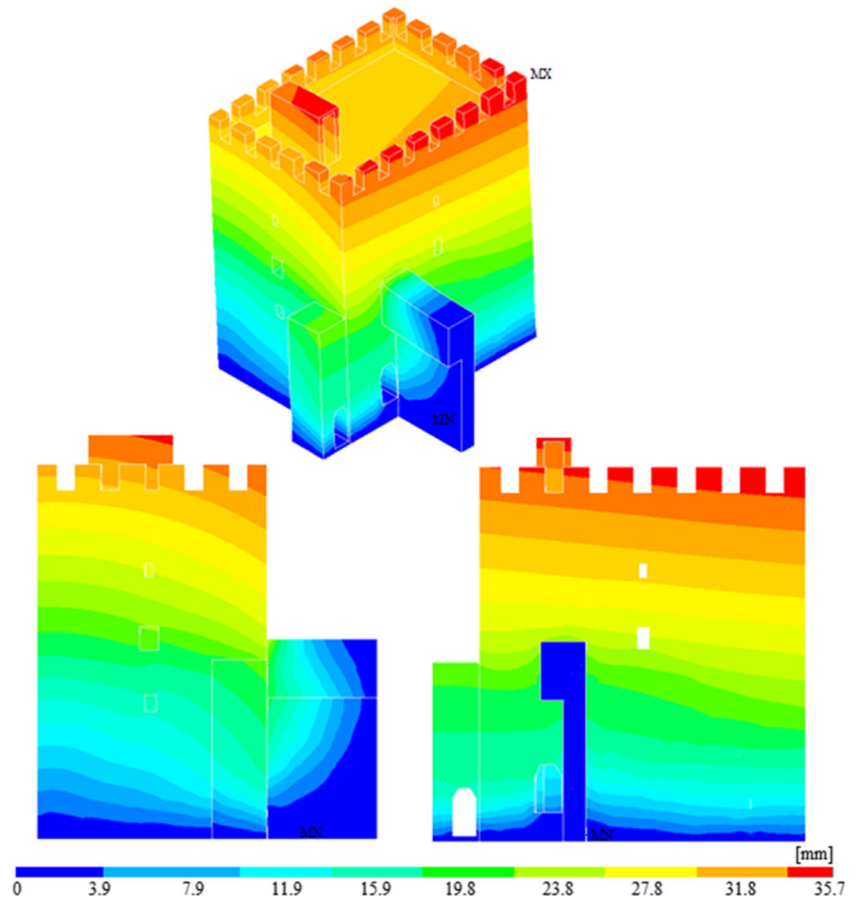**Table 5** Yield criterion and failure surface setting

Drucker-Prager criterion		Willam and Warnke surface	
c	90,000 N/m^2	f_c	8,000,000 N/m^2
μ	38	f_t	150000N/m^2
φ	15	$ß_c$	0.75
		$ß_t$	0.15

c = Cohesion f_c = Uniaxial compressive strength
μ = Dilatancy angle f_t = Uniaxial tensile strength
φ = Internal friction angle $ß_c$ = Shear transfer coeff. Close cracks
  $ß_t$ = Shear transfer coeff. Open cracks

characteristics experimentally. Linear and nonlinear time-history seismic analyses were carried out based on the Kocaeli 1999 earthquake record. The stress results of the seismic analyses were compared with the Turkish Earthquake Code requirements. The following conclusions are drawn from the study:

Experimental and Numerical Modal Analyses

• The first three experimental frequencies were obtained between 4 and 7 Hz.

• The first three numerical frequencies were obtained between 5 and 10 Hz.

• Experimental and numerical mode shapes of the bastion were obtained as transverse, longitudinal and torsional modes.

• Maximum difference between the experimental and numerical frequencies was obtained as 26 %. However, the numerical and experimental mode shapes were the same.

Linear Analysis Results

• Maximum displacement was obtained as 7.8 mm at the upper part of the bastion.

• Maximum and minimum principal stresses occurred on the later additions to the main structure. The maximum and minimum principal stresses which occurred on these elements were 4.56 MPa and 6.04 MPa, respectively.

• Maximum and minimum principal stresses on the element's joints were calculated as 2.63 MPa and 5.0 MPa, respectively. These points occurred only on small localized areas.

Fig. 17 Contour diagrams of the maximum displacements from nonlinear seismic analysis

Fig. 18 Contour diagrams of the maximum and minimum principal stresses from nonlinear seismic analysis

a) Maximum principal stresses

b) Minimum principal stresses
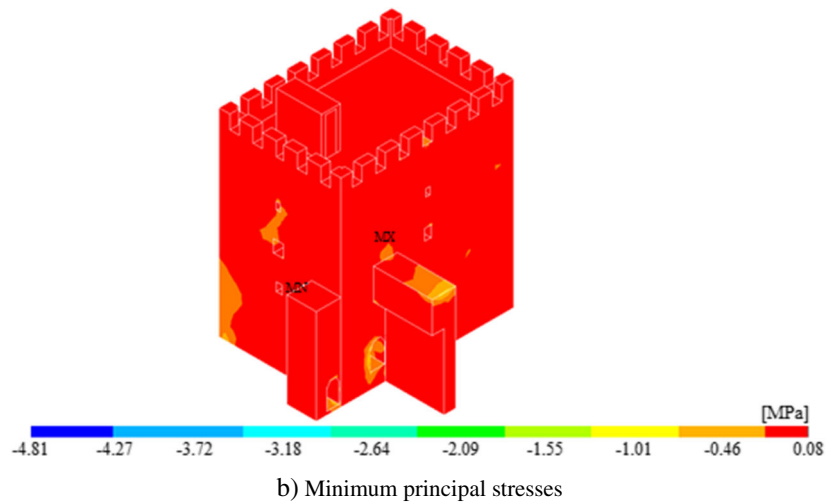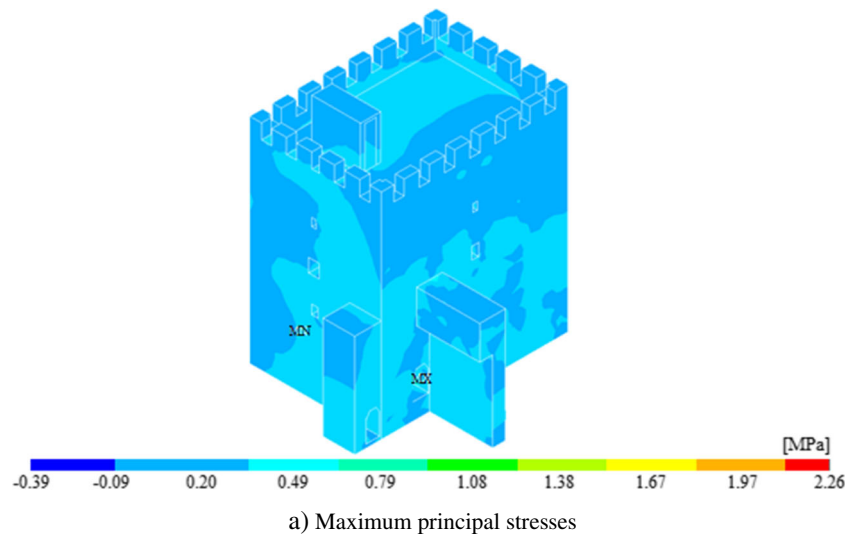
- The maximum and minimum principal stresses in the main structural elements of the bastion were obtained as 0.93 MPa and 0.90 MPa, respectively.
- The maximum and minimum principal strains were obtained as 10.59E-4 and 19.47E-4, respectively.
- The minimum principal stresses on the bastion were generally lower than the code requirements. However, the maximum principal stresses exceeded the code requirements at some points.

Nonlinear Analysis Results

- The maximum displacement was obtained as 35.7 mm at the upper part of the bastion.
- Maximum principal stress occurred on the RC floor, with a value of 2.26 MPa. The rest of the bastion had a maximum 0.49 MPa stress value.

- Minimum principal stress occurred on the RC floor with a value of 4.81 MPa. Apart from this localized point, these stresses did not exceed the value of 1.01 MPa.
- Maximum and minimum principal strains were obtained as 15.74E-3 and 2.53E-3, respectively. The maximum and minimum principal strains occurred between the elements.
- Cracks occurred generally at the lower part of the bastion. These were found mostly near window spaces and gates, side ramparts, RC floors, arches and vaults. The locations of these cracks are related to the direction of seismic loading. If the loading was applied in a longitudinal direction, the cracks would appear at different points.
- As expected, the trend is for the displacements and strains to increase significantly with the nonlinear analysis. Also, the nonlinear stress results were lower than for the linear analysis. The nonlinear seismic results were substantially different from the linear analysis.
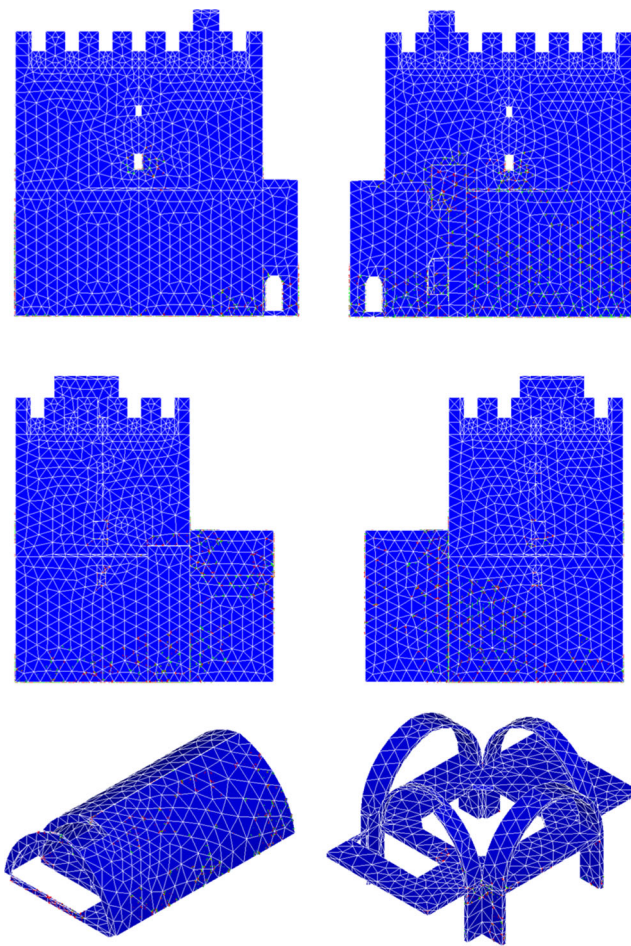
Fig. 19 Crack distributions obtained from the nonlinear seismic analysis

The bastion was originally built with arches, vaults and walls designed to resist load. However, in the last century some additional elements were added, such as an elevator, RC floors and steel columns, and these affected the structural behavior of the bastion substantially. As the results show, most of the stresses occurred on localized points between those elements. There is not any regular stress distribution on these elements of the structure because of the additions. This situation causes a general weakening in the seismic behavior of the

Table 6 Comparison of the linear and nonlinear seismic analyses results

Parameters	Updated model-seismic analyses		
	Linear	Nonlinear	*Diff.(%)*
Maximum displacement(mm)	7.8	35.7	*+357*
Maximum principal stress (MPa)	4.56	2.26	*-50*
Minimum principal stress (MPa)	6.04	4.81	*-20*
Maximum principal strains	10.59E-4	15.74E-3	*+1386*
Minimum principal strains	19.47E-4	2.53E-3	*+30*

bastion. Therefore this case clearly illustrates the importance of taking these factors into consideration in the restoration of historic masonry structures.

Historic masonry structures are an important part of our cultural heritage, and must be protected against destructive effects such as seismic actions. Determining the seismic behavior of these structures is quite difficult, especially using experimental methods. Therefore, FE analyses are used to determine seismic behaviors. Because of the unpredictable nature of factors such as material characteristics, boundary conditions and meshing in FE modeling, a true representation of the actual behavior of the structure under real conditions may not be achievable. Therefore, FE models should be updated using experimental testing methods such as the ambient vibration test. It is intended that, in this case, a future study will provide an updated FE model of the bastion using ambient vibration testing.

References

1. Parisi F, Augenti N (2013) Earthquake damages to cultural heritage constructions and simplified assessment of artworks. Eng Fail Anal 34:735–760. doi:10.1016/j.engfailanal.2013.01.005
2. Toker S, Ünay A (2004) Mathematical modeling and finite element analysis of masonry arch bridges. Gazi Univ J Sci 17(2):24–25
3. Lourenço PB, Roque JA (2006) Simplified indexes for the seismic vulnerability of ancient masonry buildings. Constr Build Mater 20(4):200–208. doi:10.1016/j.conbuildmat.2005.08.027
4. Ren WX, Penga X, Lina Y (2005) Experimental and analytical studies on dynamic characteristics of a large span cable-stayed bridge. Eng Struct 27(4):535–548. doi:10.1016/j.engstruct.2004.11.013
5. Sevim B, Bayraktar A, Altunişik AC, Atamtürktür S, Birinci F (2011) Finite element model calibration effects on the earthquake response of masonry arch bridges. Finite Elem Anal Des 47(7):621–634. doi:10.1016/j.finel.2010.12.011
6. Saisi A, Gentile C, Guidobaldi M (2015) Post-earthquake continuous dynamic monitoring of the Gabbia tower in mantua, Italy. Constr Build Mater 81:101–112. doi:10.1016/j.conbuildmat.2015.02.010
7. Altunisik AC, Kanbur B, Genc AF (2015) The effect of arch geometry on the structural behavior of masonry bridges. Smart Struct Syst 16(6):1069–1089. doi:10.12989/sss.2015.16.6.1069
8. Altunışık AC, Bayraktar A, Sevim B, Birinci F (2011) Vibration-based operational modal analysis of the Mikron historic arch bridge after restoration. Civ Eng Environ Syst 28(3):247–259. doi:10.1080/10286608.2011.588328
9. Milani G, Lourenço PB (2012) 3D non-linear behavior of masonry arch bridges. Comput Struct 110:133–150. doi:10.1016/j.compstruc.2012.07.008
10. Bayraktar A, Türker T, Sevim B, Altunışık AC, Yıldırım F (2009) Modal parameter identification of Hagia Sophia bell-tower via ambient vibration test. J Nondestruct Eval 28(1):37–47. doi:10.1007/s10921-009-0045-9
11. Peña F, Lourenço PB, Mendes N, Oliveira DV (2010) Numerical models for the seismic assessment of an old masonry tower. Eng Struct 32(5):1466–1478. doi:10.1016/j.engstruct.2010.01.027

12. Carpinteri A, Invernizzi S, Lacidogna G (2005) In situ damage assessment and nonlinear modelling of a historical masonry tower. Eng Struct 27(3):387–395. doi:10.1016/j.engstruct.2004.11.001

13. Dogangun A, Acar R, Sezen H, Livaoglu R (2008) Investigation of dynamic response of masonry minaret structures. Bull Earthq Eng 6(3):505–517. doi:10.1007/s10518-008-9066-5

14. Bayraktar A, Altunişik AC, Sevim B, Türker T (2011) Seismic response of a historical masonry minaret using a finite element model updated with operational modal testing. J Vib Control 17: 129–149. doi:10.1177/1077546309353288

15. Seker BS, Cakir F, Dogangun A, Uysal H (2014) Investigation of the structural performance of a masonry domed mosque by experimental tests and numerical analysis. Earthquakes Struct 6(4):335–350. doi:10.12989/eas.2014.6.4.335

16. Cakir F, Seker BS, Durmus A, Dogangun A, Uysal H (2015) Seismic assessment of a historical masonry mosque by experimental tests and finite element analyses. KSCE J Civ Eng 19(1):158–164. doi:10.1007/s12205-014-0468-4

17. Betti M, Vignoli A (2008) Assessment of seismic resistance of a basilica-type church under earthquake loading: modelling and analysis. Adv Eng Softw 39(4):258–283. doi:10.1016/j.advengsoft.2007.01.004

18. Lourenço PB, Trujillo A, Mendes N, Ramos LF (2012) Seismic performance of the St. George of the Latins church: Lessons learned from studying masonry ruins. Eng Struct 40:501–518. doi:10.1016/j.engstruct.2012.03.003

19. Brandonisio G, Lucibello G, Mele E, De Luca A (2013) Damage and performance evaluation of masonry churches in the 2009 L'Aquila earthquake. Eng Fail Anal 34:693–714. doi:10.1016/j.engfailanal.2013.01.021

20. Minghini F, Milani G, Tralli A (2014) Seismic risk assessment of a 50 m high masonry chimney using advanced analysis techniques. Eng Struct 69:255–270. doi:10.1016/j.engstruct.2014.03.028

21. Kamai R, Hatzor YH (2008) Numerical analysis of block stone displacements in ancient masonry structures: a new method to estimate historic ground motions. Int J Numer Anal Met 32(11):1321–1340. doi:10.1002/nag.671

22. Cacciotti R, Lourenço PB (2014) Structural assessment of the sixteenth century coastal watchtowers in the defense system of the pontifical state. Masonry International 27:1–9

23. Tilocca AR, Ferracuti B, Mazzotti C, Bovo M (2015) Seismic vulnerability assessment of a historical masonry building: Pandone Castle. Environ Energy Struct Monit Syst (EESMS), IEEE:174–179

24. Tiberti S, Acito M, Milani G (2016) Comprehensive FE numerical insight into finale Emilia Castle behavior under 2012 Emilia Romagna seismic sequence: damage causes and seismic vulnerability mitigation hypothesis. Eng Struct 117:397–421. doi:10.1016/j.engstruct.2016.02.048

25. Milani G, Esquivel YW, Lourenço PB, Riveiro B, Oliveira DV (2013) Characterization of the response of quasi-periodic masonry: geometrical investigation, homogenization and application to the Guimarães castle, Portugal. Eng Struct 56:621–641. doi:10.1016/j.engstruct.2013.05.040

26. Casolo S, Sanjust CA (2009) Seismic analysis and strengthening design of a masonry monument by a rigid body spring model: the "Maniace Castle" of Syracuse. Eng Struct 31(7):1447–1459. doi:10.1016/j.engstruct.2009.02.030

27. Betti M, Orlando M, Vignoli A (2011) Static behaviour of an Italian medieval castle: damage assessment by numerical modeling. Comput Struct 89(21):1956–1970. doi:10.1016/j.compstruc.2011.05.022

28. PULSE, Analyzers and Solutions, Release 11.2. Bruel and Kjaer, Sound and Vibration Measurement A/S, Denmark, 2006.

29. OMA, Release 4.0, Structural Vibration Solution A/S, Denmark, 2006.

30. Allemang RJ (2003) The modal assurance criterion: twenty years of use and abuse. Sound Vib 37:14–23

31. ANSYS (2013) Swanson analysis system. Pennsylvania, U.S.A.

32. Saloustros S, Pelà L, Roca P, Portal J (2015) Numerical analysis of structural damage in the church of the Poblet monastery. Eng Fail Anal 48:41–61. doi:10.1016/j.engfailanal.2014.10.015

33. Betti M, Vignoli A (2008) Modelling and analysis of a Romanesque church under earthquake loading: assessment of seismic resistance. Eng Struct 30(2):352–367. doi:10.1016/j.engstruct.2007.03.027

34. Betti M, Vignoli A (2011) Numerical assessment of the static and seismic behaviour of the basilica of Santa Maria all'Impruneta (Italy). Constr Build Mater 25(12):4308–4324. doi:10.1016/j.conbuildmat.2010.12.028

35. Turkish Earthquake Code (2007) Specification for buildings to be built in seismic zones. Ministry of Public Works and Settlement. In: General Directorate of Disaster Affairs. Earthquake Research Department, Ankara, Turkey

36. Can H, Kubin J, Ünay Aİ (2012) Seismic behavior of historical masonry buildings with irregular geometry. J Fac Eng Archit Gaz 27(3):679–686

37. Akan AE (2010) Determination of structural performance of timber pillared historical mosques by finite element analysis. SDU Intern Technol Sci 2(1):41–54

38. PEER Pacific Earthquake Engineering Research Center. University of California, Berkeley, CA

39. Betti M, Orlando M, Vignoli A (2006) Modelling and analysis of an Italian medieval castle under earthquake loading: Diagnosis and strengthening. In: Lourenço PB, Roca P, Modena C, Agrawal S (eds) . Structural Analysis of Historical Constructions, New Delhi

40. Betti M, Galano L (2012) Seismic analysis of historic masonry buildings: the vicarious palace in Pescia (Italy). Buildings 2(2): 63–82